

Which factors determine the optimal pedaling rate in sprint cycling?

A. J. “KNOEK” VAN SOEST and L. J. RICHARD CASIUS

Faculty of Human Movement Sciences, Free University, Amsterdam, THE NETHERLANDS

ABSTRACT

VAN SOEST, A. J., and L. J. R. CASIUS. Which factors determine the optimal pedaling rate in sprint cycling? *Med. Sci. Sports Exerc.*, Vol. 32, No. 11, pp. 1927–1934, 2000. **Introduction:** Mechanical power output in sprint cycling depends on pedaling rate, with an optimum at around 130 revolutions per minute (rpm). In this study, the question is addressed if this optimal pedaling rate can be understood from a Hill-type description of muscular dynamics. In particular, it is investigated how 1) the power–velocity relationship that follows from Hill’s force-velocity relationship and 2) activation dynamics (from the perspective of which the optimal pedaling rate is near-zero) affect the optimal pedaling rate. **Methods:** A forward dynamics modeling/simulation approach is adopted in this study. The skeletal model is a 2D linkage of rigid segments; it is actuated by eight Hill-type “muscles.” Input of the model is the neural stimulation of the muscles, output is the resulting movement and variables dependent thereupon, such as pedal forces. For a wide range of isokinetic pedaling rates, the neural stimulation is optimized with respect to the average mechanical power output. **Results:** Correspondence between experimental data and simulation results regarding 1) the (pedaling-rate dependent) muscle phasing, 2) pedal forces, and 3) the power-pedaling rate relationship is good. At the optimal pedaling rate predicted by the model (120 rpm), muscles contract at velocities well below those that maximize their power output. Finally, when a model is considered that lacks activation dynamics, it is found that both the optimal pedaling rate and the maximal power output increase substantially. **Discussion:** From the results pertaining to the standard model, it is concluded that the optimal pedaling rate is not uniquely specified by the power–velocity relationship of muscle, as suggested in literature. From the results pertaining to the model lacking activation dynamics, it follows that activation dynamics plays a surprisingly large role in determining the optimal pedaling rate. It is concluded that the pedaling rate that maximizes mechanical power output in sprint cycling follows from the interaction between activation dynamics and Hill’s power–velocity relationship. **Key Words:** HUMAN, MUSCLE, BIOPHYSICS, BIOMECHANICS, MODELING, OPTIMIZATION

B iomechanical modeling of the human musculoskeletal system and simulation of the behavior of that system in complex movements can contribute to our understanding of the relationship between musculoskeletal properties and task performance. In this study, such a modeling/simulation approach, in which the movement is calculated from the neural input to muscles, is applied to the task of cycling. An interesting aspect of cycling is that through employment of a gearing system, subjects may select their pedaling rate (usually expressed in revolutions per minute, rpm) independently from bicycle velocity and thus from the “mechanical power output” (i.e., the average mechanical power delivered to the crank). Regarding submaximal steady state cycling under aerobic conditions, it is well documented that the pedaling rate selected by well-trained subjects is quite consistently in the order of 90–100 rpm when the required mechanical power output is substantial. On the other hand, the pedaling rate at which oxygen consumption is minimal for a fixed mechanical power output is much lower (e.g., (17)). Despite recent attempts (e.g.,

(20)), it is currently unclear how mechanical and metabolic factors contribute to the “objective function” that determines the choice of pedaling rate during high-intensity submaximal steady state cycling.

The objective function in sprint cycling is less ambiguous than in submaximal steady state cycling. In sprint cycling, the goal is simply to maximize the mechanical power output. Experimentally, it has been observed that this mechanical power output can be sustained for a very short period of time only (e.g., 5 s) and that the pedaling rate at which this mechanical power output is maximal is approximately 120–130 rpm (e.g., (1)). Under the assumption that neither local muscle fatigue nor central physiological processes constrain performance within the short period of time considered, the contractile properties of muscle fully determine the achievable mechanical power output, and its dependence on pedaling rate. In this study, we will investigate if the relationship between pedaling rate and mechanical power output in sprint cycling can be understood from a highly simplified model of the musculoskeletal system. As variables that need to be considered in answering this question are not experimentally accessible, a forward dynamics modeling/simulation approach will be used.

Which musculoskeletal properties, then, influence the optimum pedaling rate in sprint cycling? The first and foremost candidate factor is the power–velocity relationship

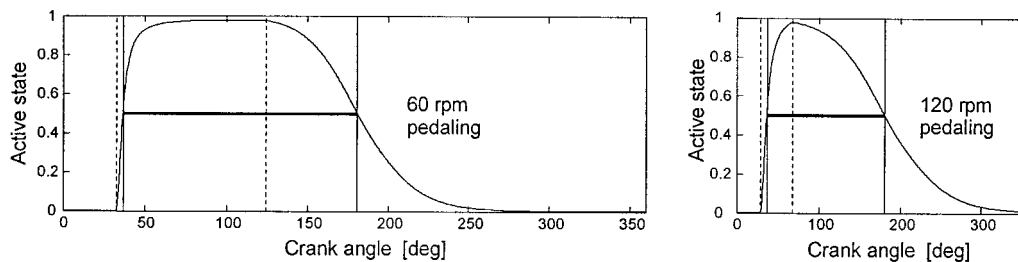


Figure 1—Schematic illustration of the effect of activation dynamics on the relation between pedaling rate and STIM switching. Active state is represented as a function of crank angle (top dead center = 0°) for a hypothetical muscle, during 60 rpm pedaling (left panel) and 120 rpm pedaling (right panel). Horizontal axes are scaled in such a way that horizontal spacing in terms of time is equal for both panels. The thick horizontal bar that is bordered by thin vertical lines represents the hypothetical range of crank angles in which the hypothetical muscle shortens. Note that this range is assumed to be identical for all pedaling rates. The dashed vertical lines represent the crank angles at which STIM switching should occur in order to make active state equal to 0.5 at the crank angles where the muscle-tendon complex velocity changes sign.

that follows from the Hill-type description of contraction dynamics used in this study. In terms of a Hill-type muscle model, contraction dynamics describes how contractile element shortening velocity depends on contractile element length, active state (as defined in (7)) and force. The essential component in this description is the force-velocity relationship that is based on the classical descriptive model of the concentric force-velocity relationship at optimum length as formulated by Hill (13):

$$(F + a) \cdot (v + b) = (1 + a) \cdot b \quad (1)$$

where F is contractile element force (relative to maximal isometric force F_{\max}), v is contractile element shortening velocity (relative to contractile element optimum length $L_{ce(\text{opt})}$; note that $v < 0$ during shortening), and a ($a > 0$) and b ($b < 0$) are parameters. From (1), it follows that the mechanical power P (in $W \cdot F_{\max}^{-1} \cdot L_{ce(\text{opt})}^{-1}$) that flows from the muscle to its environment depends on contractile element shortening velocity in the following way:

$$P(v) = v \cdot (a \cdot v - b) \cdot (v + b)^{-1} \quad (2)$$

From equation (2) it is easily derived that power is maximal when v equals v_{opt} , with

$$v_{\text{opt}} = b \cdot ((1 + 1/a)^{0.5} - 1) \quad (3)$$

For typical values of the parameters a and b , v_{opt} is about 0.3 times the maximal velocity of shortening. As pedaling rate directly affects the shortening velocity of muscle fibers, the pedaling rate that is optimal from the perspective of the power-velocity relationship is the one that allows as many muscles as possible to actively contract close to the velocity at which power production is maximal (v_{opt} in equation (3)). Indeed, some authors have interpreted the optimal pedaling rate in sprint cycling as indicative of the optimal fiber shortening velocity (e.g., (19)).

A second factor that has an impact on the optimal pedaling rate in sprint cycling is what is usually referred to as “activation dynamics”: the process of calcium release and reuptake from the sarcoplasmic reticulum. This process is usually modeled as a first-order process with the time constant for activation smaller than that for deactivation (28). As a consequence of activation dynamics, it is impossible for a muscle going through stretch-shortening cycles to have

full active state all the way through the shortening phase and zero active state all the way through the lengthening phase. It was shown by Caiozzo and Baldwin (4), who studied work output during sinusoidal length changes in stimulated rat soleus muscle, that work output was less than predicted on the basis of the force-length-velocity relationship; most importantly, they found that the work deficit increased with the frequency of sinusoidal length change. Translated to the cycling situation, the mechanism involved is illustrated in Figure 1 and described for the deactivation process here. If we want the active state of the muscle to have a particular value (set arbitrarily to 0.5 in Fig. 1) once it starts to lengthen, it has to be deactivated a certain amount of time before it actually starts lengthening. As a result, part of the concentric length change occurs while active state is submaximal, which negatively affects the potential for power production. At a higher pedaling rate (Fig. 1, right panel), shortening velocity is higher and therefore a larger part of the concentric length change occurs while active state is submaximal. Consequently, the potential for power production decreases as pedaling rate is increased: from the perspective of activation dynamics, the optimal pedaling rate is zero (!), a conclusion that is in line with the experimental findings of Caiozzo and Baldwin (4). Another consequence of activation dynamics is that at a higher pedaling rate, muscles must be active slightly earlier in the crank cycle in order to ensure high active state levels during the concentric phase, a consequence that is supported by EMG data (e.g., (16), (18)).

A third factor is related to a peculiarity of sprint cycling: in this task, pedal forces may be so high that the upper body loses contact with the saddle, resulting in a quite different mechanical system. To circumvent this peculiarity, it was decided to take a measure in our model that is similar to the experimental measure taken by Beelen et al. (2): fixing the pelvis to the saddle.

The main aims of this study, then, are as follows. First, we want to show that the relationship between pedaling rate and mechanical power output in sprint cycling as observed experimentally can be predicted from a forward dynamics model of the musculoskeletal system. Second, we want to investigate the relative importance of activation and contraction dynamics in

determining the optimal pedaling rate. For this purpose, a forward dynamics model of the system “cyclist plus crank” will be developed, and the neural input to the muscles will be optimized with respect to mechanical power output.

METHODS

Outline of the simulation study. The model reflects the experimental setup as described by Beelen et al. (2). That is, pedaling at a fixed crank angular velocity with the aim to maximize the time average of the power transferred to the crank. The analysis is restricted to periodic behavior, that is to behavior in which the movement of a leg is identical for any two crank revolutions. As the legs can be assumed to be mechanically decoupled in this task, the model is restricted to a single leg. Values for mechanical power output are reported for two legs, assuming left-right symmetry.

Input of the forward dynamics model is the neural input to each of the muscle groups modeled; output of the model is the resulting kinematics and kinetics, from which mechanical power output can be calculated. The time-dependent neural inputs to the “muscles” that maximize the mechanical power output are identified through a range of pedaling rates. It is shown that the simple model used in this study suffices to predict the pedaling rate–power output relationship. Next, we will investigate the importance of activation and contraction dynamics in determining the optimal pedaling rate. The role of contraction dynamics is investigated by comparing fiber shortening velocities at the optimal pedaling rate to the optimal fiber shortening velocities; the role of activation dynamics is investigated by considering a second model that lacks activation dynamics.

Model of the musculoskeletal system. The model used in this study is an extended version of an existing model used in simulation studies of human vertical jumping that has been extensively described (25,29). The skeletal model is two-dimensional and consists of five rigid segments connected in frictionless hinge joints. These segments represent the crank, foot, lower leg, upper leg, and head-arms-trunk (HAT). The following kinematic constraints are imposed: 1) the end of the crank is fixed in space; 2) crank rotation is prescribed (isokinetic cycling); 3) the hip joint is fixed in space; in accordance with Price and Donne (21), the seat height was set to 0.96 times the trochanteric height; and 4) the orientation of the HAT segment is fixed. Thus, the skeletal model has two mechanical degrees of freedom, one of which (crank rotation) is kinematically prescribed. Acceleration-determining forces are the gravitational forces and the moments acting at the joints that represent the net effect of the muscle forces (see below). The Newtonian equations of motion of the skeletal model are automatically derived using MUSK (5), a software package developed at the Faculty of Human Movement Sciences, Vrije Universiteit, Amsterdam. This software package is very efficient for the current type of application.

The skeleton is actuated by eight “muscles,” representing the major muscle groups of the lower extremity. A lumped

TABLE 1. Segment parameter values.

	L	d	m	J
Crank	0.17	0.09	0.20	0.00
Foot	0.17	0.12	1.23	0.01
Lower leg	0.46	0.26	3.54	0.07
Upper leg	0.49	0.28	8.47	0.21
Trunk	0.82	0.30	55.00	3.90

L, segment length; d, distance from distal end of segment to segment center of mass; m, segment mass; J, segment moment of inertia, relative to the center of mass.

Hill-type muscle model was used to represent these muscles. It consists of a contractile element, a series elastic element, and a parallel elastic element. The latter element is present in the model but has no effect in the optimal solutions to be discussed. This model has been previously described in full detail (25). In short, contractile element length is used as the state variable, and contractile element velocity depends on active state, contractile element length, and muscle-tendon complex length. The latter follows from the relative orientation of the segments. Active state as defined in (7) is related to STIM, the one-dimensional representation of the neural input of the muscle, by first order dynamics as described in (11). Thus, in total the muscle model is of second order: a first order model for activation dynamics and a first order model for contraction dynamics. Muscles included in the model are gluteal muscles, hamstrings, iliopsoas, vasti, rectus femoris, soleus, gastrocnemius, and tibialis anterior.

The way in which muscles and skeleton are interconnected is described in (26). In short, polynomial relations between joint angle and muscle-tendon complex length have been fitted to measurements of this relation in cadaver material, following the method described in (9). These relations are used both to calculate muscle-tendon complex length from the state of the skeletal system and to transform muscle forces into net joint moments.

As mentioned earlier, a second model is used in this study that differs from the default model in that it lacks activation dynamics. Effectively, this implies that the first order differential equation for γ , the concentration of free Ca^{2+} -ions, as proposed in (11):

$$d\gamma/dt = m \cdot (c \cdot \text{STIM} - \gamma)$$

is replaced by the following algebraic equation, which represents the stationary point of the previous equation:

$$\gamma = c \cdot \text{STIM}.$$

Thus, in this model γ “jumps” to its steady state value when a step in STIM is applied, and so does active state, which depends algebraically on γ .

All parameter values for the present model are identical to those used in previous work on vertical jumping (3). As explained there, segment parameter values were derived on the basis of anthropometric measurements from six well-trained volleyball players; these values are represented in Table 1. As seat height is scaled to trochanteric height, it is unlikely that the fact that the skeletal model is somewhat taller than the average cyclist affects the conclusions of this study. Regarding activation dynamics, the parameter values

TABLE 2. Muscle parameter values.

	$L_{ce(opt)}$ (m)	F_{max} (N)	L_{slack} (m)	d_{ankle} (m)	d_{knee} (m)	d_{hip} (m)
Tibialis anterior	0.087	1200	0.317	0.037		
Soleus	0.055	3000	0.246	-0.038		
Gastrocnemius	0.055	1500	0.382	-0.038	-0.014	
Vasti	0.093	5250	0.160		0.042	
Rectus femoris	0.081	1750	0.340		0.042	0.035
Gluteus max	0.200	2750	0.150			-0.062
Biceps femoris	0.104	2200	0.370		-0.026	-0.077
Iliopsoas	0.102	4000	0.115			0.050

$L_{ce(opt)}$, contractile element optimal length, based on sarcomere counts (Huijing, personal communication); F_{max} , contractile element maximal isometric force, based on physiological cross-sectional area; L_{slack} , series elastic element slack length; d_{ankle} , d_{knee} , d_{hip} , moment arm at ankle, knee, and hip joints; for soleus and gastrocnemius, for which moment arms depend on joint angle, values averaged over the crank cycle are reported.

for fast muscle given in (11) were used, on the reasoning that all motor units of the mixed-fiber-type human muscles are recruited in the sprint task considered in this study. Force-velocity parameter values (relative to F_{max} and $L_{ce(opt)}$, respectively) were $a = 0.41$ and $b = 5.2 \text{ s}^{-1}$. These values are in the range of values reported for human type IIb muscle fibers. Again, this choice of values is based on the reasoning that in the sprint task considered we have full recruitment. Contractile element optimum lengths (calculated from the number of sarcomeres in series), the polynomial coefficients that describe how origin-insertion length and moment arm depend on joint angle, and the ratios of maximal isometric muscle forces within the same functional group (e.g., $F_{max(vasti)}/F_{max(recfem)}$), which are assumed to be identical to the ratios of the PCSAs, were all based on measurements in a single set of cadavers. Absolute values for maximal isometric forces were taken from (3) and are thus representative for the volleyball players participating in that study. Series elastic element slack lengths were obtained by optimizing the fit between model-predicted and experimentally obtained joint-angle–net joint moment relationships. Relative elongation of the series elastic element at maximal isometric force was set at 0.04. Values for muscle specific parameters are given in Table 2.

The model is mathematically described by a system of coupled nonlinear first order ordinary differential equations. Given the initial state and given the independent control signals $STIM(t)$, the resulting movement is obtained through numerical integration. Numerical integration was performed using a variable-order variable-stepsize Adams-Bashford predictor Adams-Moulton corrector integration algorithm (24).

Formulation of the optimization problem; optimization algorithm; computational demands. Muscles were assumed to be maximally stimulated during part of the crank revolution and to receive no stimulation during the remainder of the crank cycle. In other words, the $STIM$ pattern for any muscle can be characterized by two parameters. To ensure periodicity of the behavior, a penalty term related to revolution-to-revolution variations in mechanical power output (ΔP_{ext}) and values of state variables (Δx) was

TABLE 3. Optimal STIM switching at 120 rpm pedaling.

	TA	SOL	GAS	VAS	REC	GLU	HAM	ILI
On (°)	174	11	23	332	307	11	41	167
Off (°)	270	85	113	20	4	74	116	267

“On” and “Off” refer to the crank angles at which $STIM$ is switched on and off, respectively.

added to the objective function. Thus, the objective function to be minimized was:

$$H = -P_{ext} + \sum (c_1 \cdot \Delta x_i^2) + c_2 \cdot \Delta P_{ext}^2$$

with all $c_1 > 0$ and $c_2 > 0$.

It was heuristically found that quick convergence onto the periodic solution was improved by adding the initial values of the state variables to the vector of parameters to be optimized, thus increasing the dimension of optimization space to 34.

A genetic algorithm was used to solve the optimization problem. In this algorithm, a value of the vector of optimization parameters is represented by a bitstring, the “chromosome.” The optimization is started by randomly producing 100 chromosomes and proceeds by gradually improving the quality of the chromosomes (i.e., the value of the objective function) through a process of variation and selection. The following rule for termination of optimizations was used: each optimization ran for at least 2000 generations (200,000 evaluations of the objective function); if the best chromosome was not outperformed during 100 subsequent generations, the optimization was terminated. All optimizations were performed twice independently as a further check on convergence. In most cases, the maximal power output obtained when rerunning an optimization was within 2% of the original value. Separate optimizations were carried out for pedaling rates ranging from 60 rpm to 240 rpm.

The computational demands to be dealt with in this study were significant. A single evaluation of the objective function for the cycling model at 120 rpm takes approximately 9 s of CPU time on a 120-MHz pentium CPU; consequently, an optimization requires about 500 h. Fortunately, the genetic algorithm is perfectly suited for parallelization; optimizations were typically performed using 30 CPUs in parallel.

RESULTS AND DISCUSSION

Is the detailed behavior in the optimal solution similar to experimental data? As the amount of experimental data on sprint cycling is limited, we will proceed by showing a number of detailed results and relate these to data of both sprint and submaximal steady state cycling. First of all, let us look at the crank angles at which $STIM$ switches. In Table 3, optimal $STIM$ switching as a function of crank angle is shown for all muscles for 120 rpm cycling. Generally, correspondence with both EMG reports (15) and with simulation results (22) is good. The only systematic difference is that, in the present model, muscles tend to be deactivated somewhat early. This difference may be due to the activation dynamics model used (11). In this model,

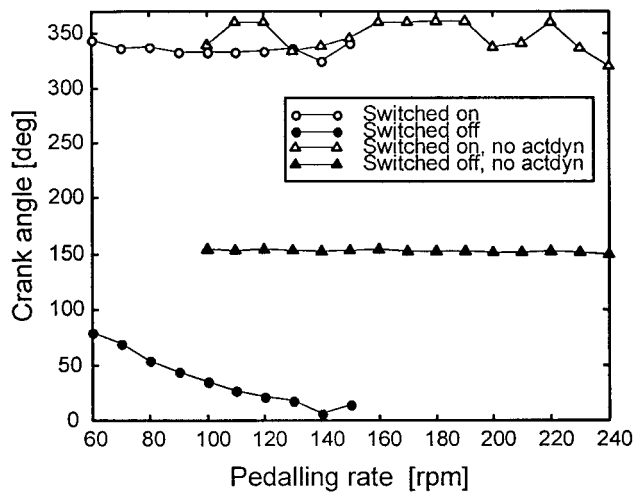


Figure 2—Crank angles (top dead center = 0°) at which vasti are switched on (open symbols) and off (solid symbols) as a function of pedalling rate, for the standard model (circles) and for the model lacking activation dynamics (triangles). Note that the results at different pedalling rates are found from independent optimizations. See text for details.

calcium dynamics is described as a linear first order system; active state is algebraically related to Ca^{2+} concentration. The latter relation is highly nonlinear and saturates at quite low values of calcium concentration. As can be seen from Figure 1, this results in a steep increase in active state upon STIM being switched on, whereas upon STIM being switched off it takes quite some time before active state starts to decrease. When active state itself is linked to STIM through linear first order dynamics, as is done for example in (22) and in the model proposed in (12), STIM would have been found to switch off later in the crank cycle. Further discussion of the merits of different models of activation dynamics goes beyond the scope of this paper.

A related topic is the relation between the STIM pattern and pedalling rate. As mentioned in the introduction, it is well documented that muscles are active earlier in the crank cycle as pedalling rate increases. In Figure 2, it is shown for the vasti group how the crank angle at which STIM switches changes with pedalling rate. It is reassuring to find that the experimental result is reproduced in the STIM switching as obtained through optimization. Note that the slope of the two curves in this figure is different: whereas the crank angle at which the muscles are switched on depends very slightly on pedalling rate, the dependence on pedalling rate for deactivation is much more pronounced. This can be understood from the fact that activation is modeled to be faster than deactivation (11,28).

Finally, in Figure 3 the pedal force is shown as a function of crank angle for 120 rpm sprint cycling, both for the optimal model solution, and for a typical experimental subject for which three successive revolutions are shown (experimental data kindly provided by Dr. A. Beelen). Comparison of simulation results and experimental data leads us to the conclusion that (1) both the shape and the magnitude of the tangential, power-producing component of the pedal force are predicted remarkably well, and that (2) the same is

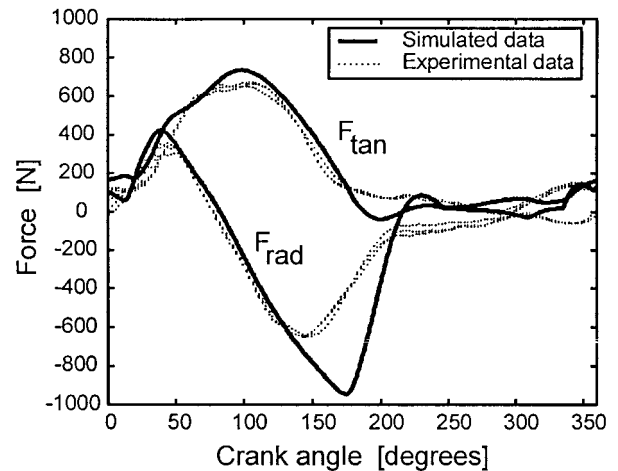


Figure 3—Tangential component F_{tan} and radial component F_{rad} of the force exerted on the pedal as a function of crank angle (top dead center = 0°) as obtained in the optimal solution for 120 rpm sprint cycling (solid curves). Dotted curves represent three subsequent revolutions by a typical subject pedaling at the same rate in the experimental study of Beelen and Sargeant (1).

true for the radial component of the force, except for crank angles around bottom dead center. The latter difference may well be due to simplifications in the model used. Alternatively, it may indicate that, even though from a mechanical point of view a high radial force is in no way detrimental to mechanical power output, in reality subjects are inclined to “penalize” high radial forces.

In conclusion, the detailed behavior pertaining to the optimal solution of the model is similar to experimental data, to the extent that it is reasonable to use the model to study the mechanics of cycling.

Can the relation between pedaling rate and mechanical power output in sprint cycling be predicted from a simple model of the musculoskeletal system? In Figure 4, the results of all optimizations are combined to yield a maximal power versus pedalling rate curve. For comparison, experimental data are shown for five individual subjects (experimental data kindly provided by Dr. A. Beelen). According to the modeling results, the highest mechanical power output is obtained at 120 rpm, amounting to 1076 W. The most important result from Figure 4 is that the optimal pedalling rate is perfectly located within the range of values obtained experimentally. The same is true for the highest mechanical power output. A close fit on this parameter was actually not expected, because the maximal isometric muscle forces, that are the most important subject-specific determinants of the magnitude of the mechanical output, were not tuned to the experimental subjects of Beelen et al. (see Methods section). Finally, the predicted dependence of mechanical power output on pedalling rate is located within the experimental range, except for the lowest pedalling rates, where the model slightly overestimates the mechanical power output. One might speculate that this is due to the fact that the coordination pattern of the experimental subjects is not optimal at these unusually low pedalling rates. However, instead of speculating about the cause of minor differences, we would rather

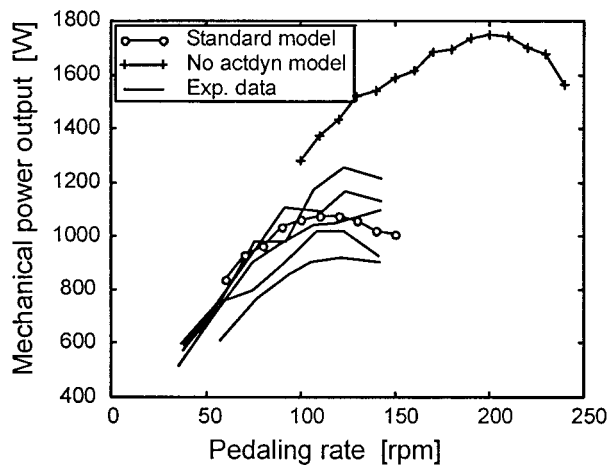


Figure 4—Mechanical power delivered to the crank as a function of pedaling rate. Solid curve marked with (○) represents optimal simulation results for the standard model; that marked with (+) represents those for the model lacking activation dynamics. Unmarked lines represent data of individual subjects from the study by Beelen and Sargeant (1).

emphasize that the degree of correspondence between experimental data and modeling results is remarkably good. We conclude that the current model of the musculoskeletal system is of sufficient detail to predict the experimentally observed relation between pedaling rate and mechanical power output in sprint cycling.

What is the relative importance of activation and contraction dynamics vis-à-vis the optimal pedaling rate?

As outlined in the introductory section, if the power-velocity relationship that can be derived from Hill's force-velocity relationship were the only factor, the optimal pedaling rate would be the one that allows as many muscles as possible to actively contract close to their v_{opt} , the velocity at which mechanical power output is maximal. On the other hand, if activation dynamics would be the only factor, the theoretically optimal pedaling rate would be zero. Thus, a first impression of the relative importance of these two processes can be obtained by comparing the contractile element contraction velocities v_{ce} at the optimal pedaling rate (120 rpm) to the corresponding v_{opt} . To be able to do this, equation (3) must be generalized to situations where active state q is submaximal, and/or contractile element length L_{ce} differs from its optimal value. In our formulation of the muscle model (for details, see (25)), v_{max} depends on L_{ce} when L_{ce} is below optimal length but does not if L_{ce} is above optimal length (27); furthermore, active state q has an effect on maximal shortening velocity at low values of q . For situations where $q > 0.3$, this leads to the following relationships for v_{opt} , which is the velocity of shortening (relative to $L_{ce(opt)}$) that results in maximal power output at the current value of L_{ce} :

$$L_{ce} > L_{ce(opt)}: v_{opt} = b \cdot ((1 + 1/a)^{0.5} - 1)$$

$$L_{ce} < L_{ce(opt)}: v_{opt} = b \cdot ((1 + F_{isom}/a)^{0.5} - 1)$$

where F_{isom} is the isometric force, relative to F_{max} , that can be delivered at the present value of L_{ce} .

Using the above relationships, in Figure 5 (top) the actual

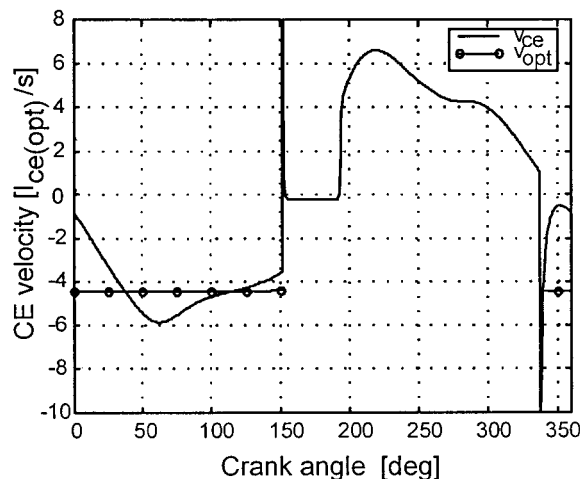
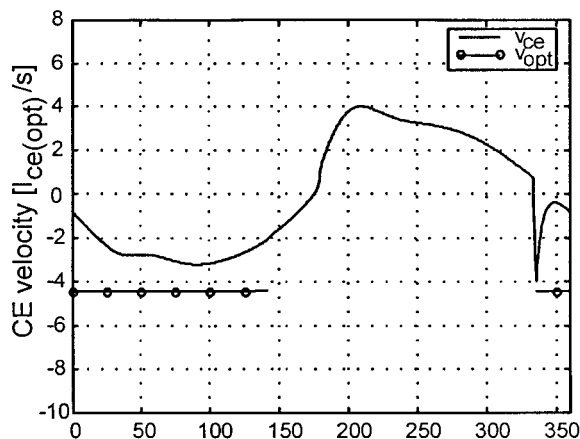


Figure 5—Top panel: v_{ce} , the CE contraction velocity, as a function of crank angle (top dead center = 0°) for the vasti group at the optimal pedaling rate (120 rpm), and v_{opt} , the CE contraction velocity that would maximize mechanical power output, which is plotted only for the part of the crank cycle where active state is larger than 0.3. Bottom panel: as with top panel, but now for the model lacking activation dynamics, at the optimal pedaling rate of 200 rpm.

values of v_{ce} (relative to $L_{ce(opt)}$) at the optimal pedaling rate are compared with the optimal ones for the muscle that contributes most to the mechanical power output: the vasti group. From this figure, it is obvious that, when active, v_{ce} of the vasti group is far too low from the perspective of the power-velocity relationship. Given that the same is true for all other major contributors to the mechanical output, it appears that contraction dynamics is not the primary factor in determining the optimal pedaling rate.

To determine whether it is activation dynamics that is responsible for the fact that the optimal pedaling rate is so much lower than would be optimal on the basis of the power-velocity relationship, a second set of optimizations was performed using a model lacking activation dynamics (see Methods section). First of all, one would expect that the crank angles at which muscles are switched on and, particularly, off, are independent of pedaling rate for this model. This expectation is confirmed by Figure 2, showing results for the vasti group. Furthermore, one would expect the optimal pedaling rate as well as the maximal mechanical power output to be higher in this model. In Figure 4, the

relation between pedaling rate and mechanical power output is plotted for this model. This relation is markedly different from the one obtained for the model including activation dynamics; the optimal pedaling rate has shifted from 120 rpm to 200 rpm, and the mechanical power output at optimal pedaling rate has increased by as much as 63%. When we now compare the actual v_{ce} at the optimal pedaling rate (200 rpm) with v_{opt} for the vasti group (Fig. 5, bottom), it is found that, when active, the optimal contraction velocity is quite closely matched by the actual one. For the phase where the active state is larger than 0.3, the average values for the actual and optimal contractile element shortening velocities, weighted for the length-dependent isometric force (which is reasonable because the potential for power production scales directly with this isometric force), are -4.33 and -4.44 , respectively. The conclusion that for this model a close agreement exists between actual and optimal CE-shortening velocities is typical for most muscles that contribute significantly to the mechanical power output. Thus, in a model lacking activation dynamics, it is indeed the power-velocity relationship that determines the optimal pedaling rate.

When we now look back at the results obtained for the original model, the conclusion can be drawn that the activation dynamics has an unexpectedly large influence on both the optimal pedaling rate and the maximal mechanical power output: as pedaling rate increases from 60 to 200 rpm, the detrimental effect of activation dynamics increases; at the same time, the potential for power production as defined by the power-velocity relation increases. Together, these opposing trends define an optimal pedaling rate at around 120 rpm.

General discussion. The results of this study show that, contrary to expectation, activation dynamics is a major determinant of the pedaling rate that maximizes mechanical power output of the model used during sprint cycling. The relevance of this conclusion depends on the validity of the model. After all, we are only interested in the characteristics of the model insofar as it represents the “real” system. In this respect, this study presents a strong case, in that both model structure and parameter values were taken from previous work on vertical jumping. Thus, the optimization results were in no way manipulated through tuning of parameter values. From the high degree of correspondence between experimental data and simulation results, we conclude that, despite its simplicity, the model structure and parameter values used in this study provide a satisfactory description of the musculoskeletal system involved in the task of sprint cycling.

Clearly, this study is not the first one to mention Hill’s power-velocity relationship and activation dynamics as factors that must be related to coordination and performance in cycling (e.g., 16, 18, 19). However, in earlier publications, activation dynamics was primarily related to experimental finding that, at higher pedaling rates, muscles tend to be activated slightly earlier (e.g., 16, 18). On the other hand, the optimal pedaling rate in sprint cycling was interpreted as a reflection of the optimum of the combined power-velocity

relationships of the muscles involved (19). In our view, this study clearly shows that the latter interpretation is unlikely to be correct; due to the low-pass characteristics of the activation dynamics, the optimal pedaling rate is bound to be lower than would be predicted from the power-velocity relations of the muscles involved.

In relation to the main conclusion of this study, it is interesting to note (e.g., (6)) that fiber type correlates both with activation and contraction dynamics: maximal shortening velocity is higher and the force-velocity relationship is less concave in type IIB fibers, and time constants for both activation and deactivation are smaller. The results of this study indicate that this covariation of parameter values for activation and contraction dynamics is essential in stretch-shortening cycles; in order to optimally exploit the power-producing capabilities of fast muscle fibers, this capability has to be matched by fast activation dynamics.

The results of this study also shed light on the fact that muscle spends a surprisingly large fraction of the total metabolic work on SR-ATPase, that is, on pumping calcium ions back into the sarcoplasmic reticulum. Combining data on isometric contractions reviewed in (10) and (14) with the classical work of Fenn (8) on isotonic contractions, the fraction of metabolic work spent on SR-ATPase during isotonic contractions can be estimated to be almost 30%. Must this be considered as a “waste” of metabolic energy? In the light of the results of this study, definitely not: during stretch-shortening cycles a fast SR calcium pump is a prerequisite for a high mechanical power output, and thus it is worthwhile to spend a fair bit of metabolic work on this process.

In this study, the focus was on the musculoskeletal determinants of the optimal pedaling rate in sprint cycling, rather than on the control strategy used to generate STIM. The correspondence observed between simulation results and experimental data does not refute the assumption implicitly made in this study that the nervous system is actually able to generate any STIM pattern desired. Indeed, the optimization of STIM resulted in adaptations of STIM phasing to changes in pedaling rate. In contrast, an interesting attempt was recently made by Raasch and Zajac (23) to formulate a simplified control strategy for cycling. According to this simplified strategy, groups of muscles that contribute to the same biomechanical function are stimulated with identical and pedaling-rate-independent phasing and in alternation with “antagonistic” groups of muscles. The strategy proposed by Raasch and Zajac is intended to be the simplest strategy that is flexible enough to accommodate a wide range of pedaling tasks. An interesting test of such a pedaling-rate-independent muscle phasing strategy would be to investigate its ability to predict the relationship between pedaling rate and power output as observed in sprint cycling.

We gratefully acknowledge Dr. Anita Beelen for giving us access to the experimental data reproduced in this paper, and Dr. A. J. van den Bogert for helpful discussions. Furthermore, we gratefully

acknowledge the financial support of Cray Research Inc. during the development of the software used in this study (Cray Research Grant 9415).

Address for correspondence: A. J. van Soest, Faculty of Human Movement Sciences, Free University van der Boechorststraat 9, NL 1081 BT Amsterdam, The Netherlands; E-mail: A_J_VAN_SOEST@FBW.VU.NL.

REFERENCES

1. BEELEN, A., and A. J. SARGEANT. Effect of fatigue on maximal power output at different contraction velocities in humans. *J. Appl. Physiol.* 71:2332–2337, 1991.
2. BEELEN, A., A. J. SARGEANT, and F. WIJKHUIZEN. Measurement of directional force and power during human submaximal and maximal isokinetic exercise. *Eur. J. Appl. Physiol.* 68:177–181, 1994.
3. BOBBERT, M. F., K. G. M. GERRITSEN, M. C. A. LITIENS, and A. J. VAN SOEST. Why is countermovement jump height greater than squat jump height? *Med. Sci. Sports Exerc.* 28:1402–1412, 1996.
4. CAIOZZO, V. J., and K. M. BALDWIN. Determinants of work produced by skeletal muscle: potential limitations of activation and relaxation. *Am. J. Physiol.* 42:C1049–C1056, 1997.
5. CASIUS, L. J. R. MUSK; a software system that supports computer simulations of large-scale realistic models of the neuro-musculo-skeletal system. Final report of Cray Research Grants Program CRG 94.15. Free University, Faculty of Human Movement Sciences, Amsterdam, Netherlands, 1995, pp. 6–50.
6. CLOSE, R. I. Dynamic properties of mammalian skeletal muscles. *Physiol. Rev.* 52:129–197, 1972.
7. EBASHI, S., and M. ENDO. Calcium ion and muscular contraction. *Prog. Biophys. Mol. Biol.* 18:123–183, 1968.
8. FENN, W. O. The relation between the work performed and the energy liberated in muscular contraction. *J. Physiol.* 58:373–395, 1924.
9. GRIEVE, D. W., S. PHEASANT, and P. R. CAVANAGH. Prediction of gastrocnemius length from knee and ankle joint posture. In *Biomechanics VI-A*, E. Asmussen and K. Jørgensen (Eds.). Baltimore: University Park Press: pp. 405–412, 1978.
10. HAAN, A. DE, J. DE JONG, J. E. VAN DOORN, P. A. HUIJING, R. D. WOITTEZ, and H. G. WESTRA. Muscle economy of isometric contractions as a function of stimulation time and relative muscle length. *Pfluegers Arch.* 407:445–450, 1986.
11. HATZE, H. *Myocybernetic Control Models of Skeletal Muscle*. Pretoria, South Africa: University of South Africa, 1981, pp. 31–42.
12. HE, J., W. S. LEVINE, and G. E. LOEB. Feedback gains for correction small perturbations to standing posture. *IEEE Trans. Aut. Contr.* 36:322–332, 1991.
13. HILL, A. V. The heat of shortening and the dynamic constants of muscle. *Proc. R. Soc.* 126B:136–195, 1938.
14. HOMSHER, E., and C. J. KEAN. Skeletal muscle energetics and metabolism. *Ann. Rev. Physiol.* 40:93–131, 1978.
15. INGEN SCHENAU, G. J. VAN, P. J. M. BOOTS, G. DE GROOT, R. J. SNACKERS, and W. W. L. M. VAN WOENSEL. The constrained control of force and position on multi-joint movement. *Neuroscience* 46:197–207, 1992.
16. MARSH, A. P., and P. E. MARTIN. The relationship between cadence and lower extremity EMG in cyclists and noncyclists. *Med. Sci. Sports Exerc.* 27:217–225, 1995.
17. MARSH, A. P., and P. E. MARTIN. Effect of cycling experience, aerobic power, and power output on preferred and most economical cycling cadences. *Med. Sci. Sports Exerc.* 29:1225–1232, 1997.
18. NEPTUNE, R. R., S. A. KAUTZ, and M. L. HULL. The effect of pedaling rate on coordination in cycling. *J. Biomech.* 30:1051–1058, 1997.
19. NEPTUNE, R. R., and W. HERZOG. The association between negative muscle work and pedaling rate. *J. Biomech.* 32:1021–1026, 1999.
20. NEPTUNE, R. R., and M. L. HULL. A theoretical analysis of preferred pedaling rate selection in endurance cycling. *J. Biomech.* 32:409–415, 1999.
21. PRICE, D., and B. DONNE. Effect in variation of seat tube angle at different seat heights on submaximal cycling performance in man. *J. Sports Sci.* 15:395–402, 1997.
22. RAASCH, C. C., F. E. ZAJAC, B. MA, and W. S. LEVINE. Muscle coordination of maximum-speed pedaling. *J. Biomech.* 30:595–602, 1997.
23. RAASCH, C. C., and F. E. ZAJAC. Locomotor strategy for pedaling: muscle groups and biomechanical functions. *J. Neurophysiol.* 82: 515–525, 1999.
24. SHAMPINE, L. F., and M. K. GORDON. Computer solution of ordinary differential equations. The initial value problem. San Francisco: W.H. Freeman, 1975, pp. 156–232.
25. SOEST, A. J. VAN AND M. F. BOBBERT. The contribution of muscle properties in the control of explosive movements. *Biol. Cybern.* 69:195–204, 1993.
26. SOEST, A. J. VAN, A. L. SCHWAB, M. F. BOBBERT, AND G. J. VAN INGEN SCHENAU. The influence of the biarticularity of the gastrocnemius muscle on vertical jumping achievement. *J. Biomech.* 26:1–8, 1993.
27. STERN, J. T. Computer modeling of gross muscle dynamics. *J. Biomech.* 7:411–428, 1974.
28. WINTERS, J. M., and L. STARK. Estimated mechanical properties of synergistic muscles involved in movements of a variety of human joints. *J. Biomech.* 21:1027–1041, 1988.
29. ZANDWIJK, J. P. VAN, M. F. BOBBERT, M. MUNNEKE, and P. PAS. Control of maximal and submaximal vertical jumps. *Med. Sci. Sports Exerc.* 32:477–485, 2000.